INTERPRETATION OF XUV SPECTROHELIOGRAMS*

HAROLD ZIRIN

Mount Wilson and Palomar Observatories, Carnegie Institution of Washington, California Institute of Technology

(Received 27 February, 1969)

Abstract. Some parameters of chromospheric structure are drawn from recently published XUV spectroheliograms. The He II emission above the limb arises from the small amount of He^+ still existing at 10^6 °. The larger amounts of He^+ in the cooler corona at the poles explain the polar cap absorption in λ304. The flat distribution of emission in O IV and O V, with a sharp spike at the limb, is caused by the rough structure of the chromosphere and the variable excitation in the emitting spicules. The intensity of the Ne VII lines shows that the transition zone between chromosphere and corona is very sharp.

1. Introduction

Tousey and Purcell (Tousey, 1967) have recently obtained slitless spectra of the Sun in the XUV region, which permit us to see the gross features of distribution of emission in the resonance lines emitted by the chromosphere and corona. The resolution of the Tousey-Purcell pictures (which are reproduced by Tousey, 1967, Figures 27 and 28) is high enough so that the chromospheric network is resolved, at least in the images of He II λ 304 and He I λ 584. The other, weaker lines are underexposed, and either do not have the same structure or are too lightly exposed to show it. These N.R.L. photographs are rich in information on the Sun, and their interpretation is a challenge to our understanding of solar physics. We discuss here only a few of the conclusions that may be drawn from them.

The following are salient points of the Tousey-Purcell spectroheliograms relevant to chromospheric structure:

The spectroheliogram in the He II λ 304 line is similar to one in the Ca II K line except that the limb darkened is confined to the poles, and filament absorption is weak. There is a marked absorption in the solar polar cap (SPCA). Emission of the disk in λ 304 was shown by Tousey and Purcell to come mainly from those points in the chromosphere network. The SPCA also appears in the coronal resonance lines.

The He I λ 584 line shows properties similar to λ 304, except that the SPCA is less marked.

The chromospheric lines O IV λ 555 and O V λ 630 show essentially flat distribution of emission, with a limb brightening of a factor of two beginning about $r = 0.9$. These lines do not show the SPCA. The transition zone line of Ne VII λ 465 has a sharp, narrow limb brightening and no SPCA.

Purcell and the author made microdensitometer tracings of the above lines (Figure 1). The tracings were made across the images normal to the dispersion, from position

* This research was supported by the National Aeronautics and Space Administration under Grant NASA NGR 05 002 034.

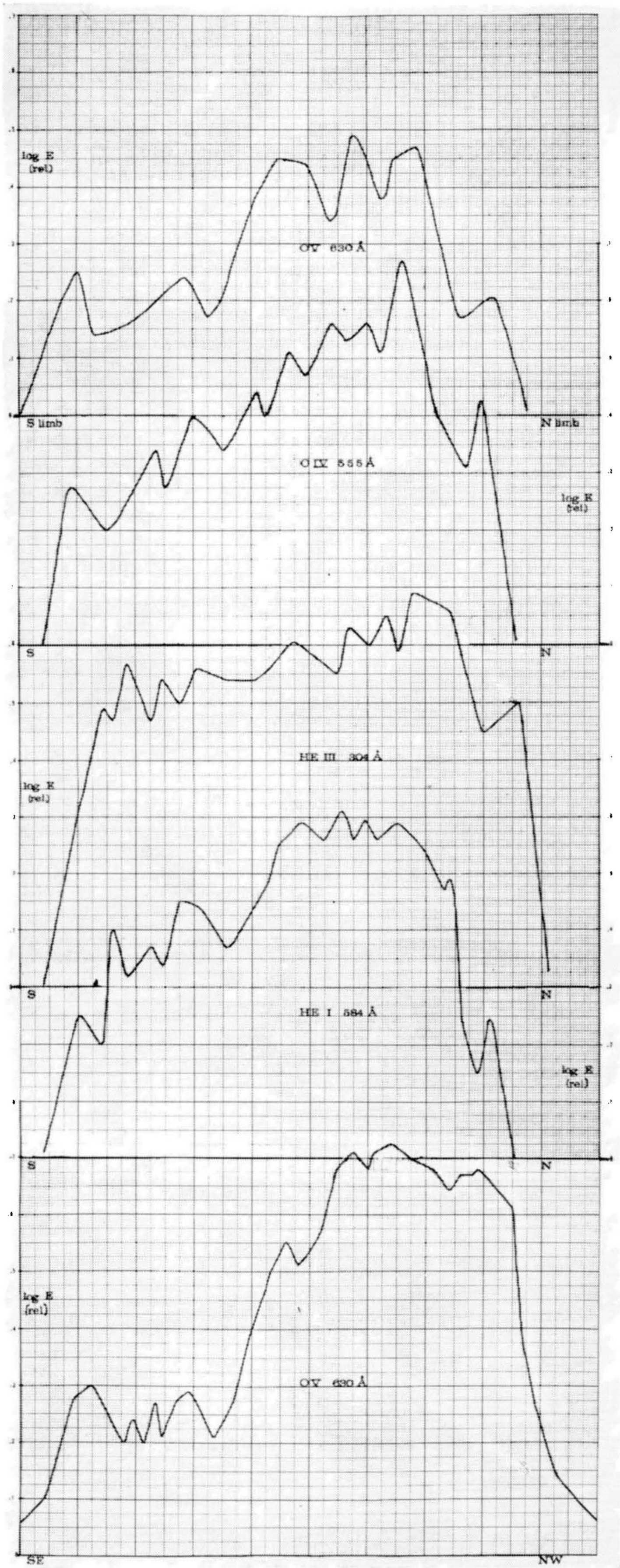

Fig. 1. Distribution of intensity across the disc in several XUV lines as measured on NRL spectroheliograms.

angles 200° to 20°. A tracing was also made across the O v image at P. A. 120°, which was also most useful because of the lack of strong lines to the long wavelength side and plage activity in this region; we therefore obtain an excellent distribution across the quiet Sun.

All the XUV lines are enhanced in the plage regions because of the higher temperature. The observed intensity there could be used to obtain a limit on the extent of the chromosphere above plages.

The slight tilt of the solar axis enables us to see the marked limb brightening in λ 304 and λ 584 away from the poles. This effect is enhanced by the presence of the nearby SPCA.

2. Intensities of Chromospheric XUV Lines

A number of authors (Zirin *et al.*, 1962; Zirin and Dietz, 1963; Pottasch, 1963; Athay, 1966) have discussed the emission of XUV lines. Certain characteristics of these lines are simple. Since they are resonance lines of low optical depth it is only the helium lines that have $\tau > 1$, but even for these τ is sufficiently small so that all quanta produced by collisional excitation escape.

The absorption coefficient in a Doppler-broadened line is:

$$
\begin{aligned}
l_0 &= 0.01497 \frac{f}{\Delta\lambda_D} = 0.00497 f \lambda \sqrt{\frac{Am_H}{2kT}} \\
&= 6.72 \times 10^{-9} f \lambda \sqrt{A} \quad \text{at} \quad 30\,000°
\end{aligned}
$$

where A is the molecular weight. The values of l_0 for the lines in question, and the number of protons $N_e L$ in the line of sight for optical depth $= 1$ are given in Table I (standard abundance values are used):

TABLE I

The adsorption coefficient and the number of protons in the line of sight

Ion Line	He II λ 304	He I λ 584	O IV λ 555	O V λ 630
l_0	1.7×10^{-14}	2.75×10^{-14}	1.5×10^{-13}	1.69×10^{-13}
$N_e L$	6.0×10^{14}	3.60×10^{14}	7.0×10^{16}	6.00×10^{16}

Observed line intensities may be used to calculate $N_e L$ for such lines (Zirin and Dietz, 1963) if we assume a spherically-symmetric atmosphere. The values obtained are so small that the lines undoubtedly come from only a fraction of the surface; otherwise the intensity would be far greater, and the line ratios in multiplets would be greatly altered.

Except for the SPCA phenomenon discussed in the next section, the behavior of the optically-deep He I and He II lines is essentially as expected. The exact amount of emission from each point in the atmosphere will depend on various non-LTE effects which, to have any meaning, must be calculated for the exact geometry of the emitting element. But the hot regions will, logically, emit more and the cool regions less so long as the optical depth is high. Thus, the emission pattern in the helium lines follows the chromospheric network. The hot regions around the edges of the network produce most of the emission. The fact that prominences in λ 304 are seen in emission at the limb, while their absorption on the disk is relatively weak, argues that the optical depth of λ 304 in prominences is so great that an excitation temperature nearly as high as that of the disk is built up.

The brightness distribution of the weaker XUV chromospheric lines is more difficult to explain. The microdensitometer tracings (Figure 1) show the peak at the limb to be about twice the quiet disk intensity, which is essentially flat except for an enhancement of at least 2 or 3 times in the active regions. This distribution recalls the 8.6 mm emission across the disk which was measured by Coates *et al.* (1959). However, the radio intensity corresponds to the surface temperature involved, whereas the lines of O IV and O V, which occur at temperatures of the order of 50 000 K, show observed brightness temperature of only 5000°. Thus, the Sun cannot be covered with an optically deep layer radiating them; the sources must be scattered, or optically thin.

Important confirmation of the optical depth of chromospheric resonance lines could be obtained from observed multiplet ratios if the data at hand were not somewhat contradictory. Hinteregger (1965) shows the $\lambda\lambda$ 788–790 lines of the O IV doublet as of nearly equal intensity. A spectrogram obtained by Detwiler *et al.* (1961) shows a ratio nearer 2:1, which suggests an optically thin line. The 780 Å region is near the limit of the Detwiler *et al.* (1961) spectrum; the measurements by Hinteregger (1965) are probably more reliable in this case. The supermultiplet $2p-2p^2$ in O IV consists of multiplets $2p\ ^2P-2p^2\ ^2D$ (790 Å) $-2p^2\ ^2S$ (610 Å) $-2p^2\ ^2P$ (555 Å); they should have the intensity ratio 5:1:9. If the lines were optically deep, the first and third should have about the same intensity, while the second should be more than one-fifth the intensity of the first. The first and third multiplets do in fact show about the same intensity, but errors of a factor of two are possible; the second multiplet would provide an excellent test, but is unfortunately hiding behind the strong Mg X line at 610 Å.

The case of O III is similarly unclear; the $\lambda\lambda$ 832 and 703 lines should have the ratio 15:9 if optically thin, but λ 832 is blended with O II. However, the total intensity of the O II and O III lines at λ 832 is only twice that of the λ 703 line; therefore it is reasonable to conclude that the O III lines have roughly equal intensity and are optically deep. A stronger argument is the presence in the XUV of many O III lines with intensities of the same order of magnitude. This suggests that the strongest lines are optically deep.

It should be noted that for the theoretical multiplet ratios to occur, not only must the emitting layer be thin, but also the overlying material. It is not clear how many photons are lost through photoionization (by these lines) of traces of neutral atoms such as H, triplet He, and neutral C, N, and O. The gradient of temperature is so steep that scattered photons may easily reach regions of un-ionized atoms in their random path through an optically deep chromosphere. This effect will be different for lines from each stage of ionization. The validity of the assumption made by most authors (including this one), that all photons produced by collisional excitation escape the chromosphere, needs critical examination.

On balance the observed multiplet ratios suggest that the carbon and oxygen chromospheric lines are optically thick, while the nitrogen lines must be optically thin. Since the integrated line intensities are measured, the optical depth must be so great that photons are lost to collisions of the second kind or photoionization, and not merely redistributed in the line.

Finally, we must bear in mind the extremely small amounts of material needed to produce the observed lines, assuming that the emitting material is at the temperature deduced from line ratios. According to Zirin and Dietz (1963), the total emission in these lines can be produced by a homogeneous optically thin layer with integrated $N_e^2 H$ less than 5×10^{25}. If the density in that layer is 10^{10}, then the height is less than 5 km. This height is so small that we must expect emission of the chromospheric XUV lines from all over the disk unless one adopts a chromospheric model in which the temperature reaches 30 000° only at coronal densities.

3. Why is the Brightness Distribution Flat?

The problem of a flat distribution of brightness across the disk is a troublesome one which already has occurred in radio astronomy.* It is clear that the flat distribution in the XUV chromospheric lines must result from an inhomogeneous or rough structure. In order to comprehend the possibilities, we sketch the distributions obtained from several limiting cases:

1. Secant brightness distributions:

a. *Optically thin, homogeneous layer of thickness H.* Brightness is proportional to path length, which varies with $\sec\theta$. At small distances D from the limb, the path length S and hence the intensity, is given by

$$S \approx H \sec\theta \qquad \text{(center of disk)}$$
$$S \approx \sqrt{H+D} - \sqrt{D} \qquad \text{(just inside the limb)}$$
$$S \approx 2\sqrt{2}\sqrt{H-D} \qquad \text{(just outside the limb)}$$

with all quantities in solar radii. The peak just outside the limb is $2\sqrt{2}/\sqrt{H}$ times the central intensity; for $H = 0.004$ this factor is 44, but sufficient resolution is needed to see it.

b. *Optically thin flat sheets* – same as 1a.

c. *Isolated thin elements of any shape. Isolated thick elements except platelets.* All these have individual emission independent of angle, but the apparent surface density increases as $\sec\theta$.

2. Flat distributions:

a. *Optically deep platelets.* These elements are defined as having smaller height

* Note added in proof: Recent data (Simon, M. and Zirin, H. – submitted to *Solar Phys.*) shows a flat brightness distribution over the quiet sun at all radio wavelengths from 3 mm to 50 cm.

than length. Their emission is independent of angle; so is the apparent fraction of the disk they cover. When their apparent separation is foreshortened to equal their height, a limb spike occurs.

b. *Thin hot layer on a rough cool surface*. The path length is limited by the roughness. A limb spike occurs when we see over the tops of the rough elements.

c. *Clumps of spicules, some cool and some hot*. Similar to 2b; although the apparent density of spicules on the disk increases toward the limb, this is balanced by the fact that the emission from those spicules (or parts thereof) that are radiating is absorbed by the cooler material in their neighbors.

The N.R.L. spectroheliograms show a close correspondence between the areas of emission in the He II λ 304 line and the Ca II K line. Thus we may accept the argument of Zirin and Dietz (1963) that the emission at this level comes predominantly from the bright flocculi and spicules located along the bright network. The λ 304 spectroheliogram has sufficient resolution to show that the network pattern is preserved toward the limb, and the surface density of bright elements increases, yet there is only slight limb brightening. This can only be due to partial obscuration of the elements by cooler chromospheric features.

Using the structure in λ 304 as a model, we may consider that the O IV and O V lines, as well as other XUV coronal lines, are emitted chiefly in the spicule bushes at the edges of the chromospheric network (the bright flocculi below are presumed to have too low a temperature). The typical spicule bush is a complex mixture of bright and dark vertical elements. Presumably the spicules, like surges, start out bright but darken as they expand. Even though their kinetic temperature may increase upwards, the sharp drop in density lowers the excitation temperature relative to the disk, particularly in a subordinate line like Hα. In the XUV lines, however, the disk background is weak, and the spicules are bright. But since the spicules are a dynamic phenomenon, they are not always bright. Some must be hot and others (presumably those in the declining phases) may be cooler. Any spicule model which carries the material from photospheric to coronal temperatures must have some range and variety of temperature. Because of the close juxtaposition of spicules in a bush, the hot elements will be obscured by the cool ones, particularly near the limb. In the disk center we see almost all of the spicules. This obscuration cancels out the secant effect and produces a uniform distribution of brightness across the disk.

Thus the spatial distribution of emission in the XUV chromospheric lines can be explained in terms of emission from the clumped distribution of spicules at the edges of the chromospheric network.

We have alluded to the dynamic nature of spicules, and the transition region in general. This fact is of the greatest importance in interpreting the intensities of the XUV lines. In any spicule, there is a change of temperature from photospheric to coronal values as it goes through the shock stage and decays. The jet-like formation that we see appears to be the locus through which material streams, with velocities considerably higher than those projected. The relative intensity of different stages of ionization will thus represent the time spent by the material in each stage of ionization as it passes through. If the material is being heated, the ionization temperature will lag behind the kinetic temperature. In any event, no steady state equilibrium formula can be used until we have a good picture of the spicule life history. The emitting transition regions are connected with isolated spicules, but the secant effect in their distribution is cancelled out as we approach the limb by absorption in the intervening spicules, parts of which are at lower temperatures. This emission is seen against a background of the emission from the thin transition layer inside the chromospheric cells which overlies a rough surface as in model 2c. In this model we have maintained the picture that the temperature rise occurs only over the spicule bushes (and above active regions). As we have pointed out in the past (Zirin and Dietz, 1963), there is at present no evidence for a general temperature increase upward in the solar atmosphere outside of the spicule bushes, except for the expectation of spherical symmetry in the coronal temperature. The absence of secant brightening in *any* transition zone line confirms the absence of a general temperature rise of any significance. Athay (1966) has shown that in a conduction model the entire transition can occur in 50 or 100 km. The actual transition height varies in time and position with the surface dynamics.

4. Self-Absorption in Helium and Hydrogen

An important result of the Rutherford theory is that an atom contains a fixed number of electrons and therefore cannot be ionized beyond a certain degree. This is particularly significant for hydrogen and helium which can only be ionized once and twice, respectively. As a result, no matter how high the temperature, all these atoms will remain in the state of relatively low ionization potential. According to Elwert's (1952) ionization formula, the ratio of one ionization stage to the next higher is given by

$$\frac{N(i+1)}{N(i)} = 2.1 \times 10^5 \frac{P(i)}{n} \left(\frac{X_H}{X_i}\right)^2 \frac{e^{-X_i/kT}}{X_i/kT}$$

where n is the principal quantum number and P is the number of ionizable electrons.

For He^+ and H, P and n are unity. If we let

$$x_i = \frac{157\,000°}{T} \frac{X_i}{X_H}$$

$$\frac{N(i+1)}{N(i)} = R(i) = 1.25 \times 10^4 \left(\frac{X_H}{X_i}\right)^2 \frac{e^{-x_i}}{x_i}$$

For high temperatures this is linear in x_i. Table II gives values of $1/R(i)$, the fraction of the remaining H or He^+, for various temperatures. We see that there are substantial amounts of He^+ and H at all temperatures. In more complex atoms, the ratio to the next stage of ionization might be the same, but all the atoms have been ionized to a much higher degree, so that the absolute number on the next higher stage is very

TABLE II

Fractions of H and He^+

T	H/H^+	He^+/He^{++}
157000	21.7×10^{-5}	$319. \times 10^{-3}$
314000	6.6×10^{-5}	18.8×10^{-3}
471000	3.7×10^{-5}	6.45×10^{-3}
628000	2.6×10^{-5}	3.48×10^{-3}
785000	2.0×10^{-5}	2.29×10^{-3}
1570000	0.88×10^{-5}	0.762×10^{-3}
3140000	0.42×10^{-5}	0.312×10^{-3}

small. The fraction He^+/He^{++} is 100 times greater than that of H/H^+ at the same temperature. Consequently, even if hydrogen is 10 times more abundant than helium, the opacities in the helium resonance lines will be at least 10 times that in the hydrogen lines.

For a fair-sized coronal condensation, $N_e = 10^{10}$, $T \approx 2 \times 10^6$ and $L = 5 \times 10^9$, so there are about 3×10^{16} He^+ ions along the line of sight. This accounts for the sizeable He II emission appearing in the N.R.L. spectroheliograms from coronal condensations at the limb; it also suggests that some coronal condensations should show absorption effects against the disk, because of the pure-scattering dilution effect. Unfortunately, most coronal condensations are seen against enhanced λ 304 plage emission; the effect is thus difficult to detect. If the plages are very much stronger than the quiet disk, there can be an apparent enhancement in λ 304 in nearby regions, owing to the scattering of λ 304 from a plage by a nearby coronal cloud (particularly one closer to the limb). This effect is seen near several plages on the N.R.L. pictures. We should expect the λ 304 line in these regions to be broader, because of its coronal origin.

At 500000°, $\tau = 1$ in Ly-α for 1.5×10^{16} H atoms, or from Table II, 5×10^{20} H^+ ions. Since a big coronal condensation has $N_H L \approx 5 \times 10^{19}$, coronal self-absorption in Ly-α is negligible. The broad absorption cores in Ly-α and Ly-β are more likely due to self-absorption in spicules and other elements of the transition zone. The observed fact that the self-absorption in Ly-α and Ly-β is strongest over quiet regions is consonant with the absence of a normal chromospheric transition region over plages. The same phenomenon was observed long ago in Ca II K.

The details of the Ly-α and β self-absorption are bound up with the complexities of chromospheric structure such as the odd fact that in Hα and Ca II K, all bright flocculi have dark spicules above them.

The SPCA effect in λ 304 can now be explained in terms of self-absorption. A lower chromospheric temperature in the polar region is ruled out because no such effect is detected in spectroheliograms pertaining to the immediately underlying chromosphere, either in Ca II K, Hα, or the lines of O IV and O V. Furthermore, the Ne VII line (λ 465) shows no SPCA, so there can be no effect in the transition zone. Thus the effect can only occur in the corona.

It would appear more likely that the corona above the poles is relatively cool, of the order of 500 000 K. This would seem plausible because of the absence of high-ionization coronal lines, and the presence of Ne VII, a low-ionization line. As a result, there is enough He^+ in the quiet corona to produce the SPCA.

Using Tables I and II, we see that for scale height 50 000 km and base density $N_e = 10^8$, there is a sizeable opacity in λ 304 even at 450 000 K. It can only contribute to a darkening of the λ 304 image, because the density is so low that the ions are all in the ground state, and the excitation temperature is thus very low. Table II shows that the λ 304 optical depth drops by a factor 10 when we go to normal coronal temperatures. Note that there should be no SPCA in Ly-α, a fact confirmed by the N.R.L. OSO II spectroheliograms.

This second explanation, although attractive, requires that there be no absorption in the He I resonance line which could only contribute for temperatures below 150 000 K. Once again, the data are insufficient.

The Gnevyšev and Gnevyšev (1954) report of D3 emission from neutral helium in the corona (not connected with prominences), has been disputed by Zirin *et al.* (1964) who showed that D3 emission could easily be produced by instrumental scattering of chromospheric D3 in the coronagraph secondary optics. If the effect were indeed coronal and not instrumental, the amount of He would be sufficient to give an SPCA in the λ 584 line. It would, in that case, be visible over the entire Sun rather than at the poles.

5. The Transition Region

Since it has been shown by Kozlovsky and Zirin (1968) that O VI is a coronal line, the Ne VII line at 465 Å remains the only true transition zone line. In contrast to the lines of higher ionization arising in the corona, which show a peak brightness just above the limb extending out into the corona, Ne VII peaks just at the limb in a thin bright ring all the way around the disk. It shows no SPCA, but the distribution on the disk is obscured by blending.

According to the recent calculations of Allen and Dupree (1967), this ion comprises a maximum of 0.3 of all neon at about 600 000°, and falls off steeply at higher and lower temperatures; this is because Ne VII belongs to the beryllium sequence and the ion Ne^{7+} has many excitable levels at all values of kT, resulting in strong dielectronic recombination.

Considering the layer in which Ne VII is emitted to have $T = 500\,000°$ and $\frac{1}{4}Ne^{6+}$, we apply the formula of Zirin and Dietz (1963):

$$\Phi = \tfrac{1}{4} \times 1.24 \frac{R_{01}^2}{a_0^2} n_e n_a T^{-1/2} H \cdot \left(E_1(\chi/kT) + e^{-\chi/kT} \ln 4\right).$$

This relation converts the observed total flux given by Hinteregger, 2×10^8 photons/cm^2/sec, to the volume emitting Ne VII. For 500 000 K, we find

$$N_e N_{Ne} H < 24 \times 10^{20}$$

or

$$N_e^2 H < 2 \times 10^{25},$$

where we have assumed $N_H = 3 \times 10^4 \ N_{Ne}$.

If we now choose various densities for the emitting layer, we get various heights, as shown in Table III.

TABLE III

Heights corresponding to varions densities of the emitting layer

N_e	H
10^{10}	0.6 km
10^9	60 km
10^8	6000 km
10^7	600000 km

We know that the density in the 600 000 K Ne^{6+} layer must exceed coronal densities, for this region underlies the corona; hence $Ne > 10^9$. Therefore the thickness of the 600 000 K layer in equatorial regions is about 100 km, explaining the sharp limb spike in the Ne VII spectroheliogram. Since the disk distribution is not known, we cannot specify if the emission comes from scattered regions or not.

Following the same procedure for the resonance lines of iron below 400 Å, we should find very different results. The many iron ions produce a great number of lines, with a total flux probably exceeding 10^{10} photons/cm^2/sec. Furthermore, N_H/N_{Fe} is about 3×10^4. Using these values, we find at a temperature of 2×10^6 K, $N_e^2 H \approx 6 \times 10^{27}$, and for $N_e \approx 10^9$, $H = 60\,000$ km, in good agreement with our knowledge of the corona. This result confirms the logic of the calculations.

In deriving the total number of atoms that might reasonably produce a certain line from the total flux of photons, we inevitably overestimate the thickness of the uniform layer involved because most of the radiation comes from the active regions. It is therefore important to note that the Zirin and Dietz (1963) calculations have in fact underestimated the extreme sharpness of the transition zone.

The exact structure inside the chromospheric network cells is still unclear. Athay (1966) has shown that under conduction equilibrium, the transition to coronal temperatures can take place in a few kilometers. Thus we should have almost no transition zone emission from those regions.

6. Summary

A number of interesting effects explain the XUV spectroheliograms. The He II emission above the limb is due to remnant He^+ in the corona. The same phenomenon, occurring in the cooler (500 000°) corona at the poles, explains the polar cap absorption in λ 304, but there is not enough hydrogen in the corona to explain the Lyman line reversals. The flat distribution of O IV and O V, with a small spike at the limb, is explained by the complex structure of spicule bushes with cooling spicules absorbing radiation from new ones. The intensity of the Ne VII lines shows that the transition region is very sharp.

Acknowledgements

I am grateful to Drs. R. N. Tousey and J. D. Purcell for the opportunity to examine their original plates, as well as stimulating discussions of this problem.

References

Allen, J. W. and Dupree, Andrea K.: 1967, *Harvard Shock Tube Lab. Sci. Rep.*, No. 24.
Athay, R. G.: 1966, *Astrophys. J.* **145**, 784.
Coates, R. J., Gibson, J. E., and Hagen, J. P.: 1959, *Astrophys. J.* **128**, 406.
Cragg, T., Howard, R., and Zirin, H.: 1963, *Astrophys. J.* **138**, 303.
Detwhiler, C. R., Garrett, D. L., Purcell, J. D., and Tousey, R.: 1961, *Ann. Geophys.* **17**, 9.
Elwert, G.: 1952, *Z. Naturforschung* **7A**, 432.
Gnevyšev, M. N. and Gnevyšev, R. S.: 1954, *Byull. Komis. po issled. Solntsa* **10**, 60.
Hinteregger, H. E.: 1965, *Space Sci. Rev.* **4**, 461.
Kozlovsky, B.-Z., and Zirin, H.: 1968, *Solar Phys.* **5**, 50.
Pottasch, S. R.: 1963, *Astrophys. J.* **137**, 945.
Simon, G. W. and White, O. R.: 1966, *Astrophys. J.* **143**, 38.
Tousey, R.: 1967, *Astrophys. J.* **149**, 239.
Zirin, H., and Dietz, R. D.: 1963, *Astrophys. J.* **138**, 664.
Zirin, H., Hall, L. A., and Hinteregger, H. E.: 1962, *Space Res.* **3**, 760.
Zirin, H., James, R., and Watson, D. K.: 1964, *Astrophys. J.* **69**, 565.